Bulletin of the Seismological Society of America, Vol. 104, No. 4, pp. 1750–1762, August 2014, doi: 10.1785/0120130201

Earthquake History of the Sumatran Fault, Indonesia, since 1892, Derived from Relocation of Large Earthquakes

by Nobuo Hurukawa, Biana Rahayu Wulandari, and Minoru Kasahara

Abstract We map the fault planes of $M \geq 7.0$ earthquakes along the Sumatran fault in Sumatra, western Indonesia, for the period since 1892. To obtain precise hypocenter locations of large earthquakes and identify fault planes of $M \geq 7.0$ earthquakes, we relocated 27 $M \geq 6.0$ earthquakes from 1921 to 2012 using the modified joint hypocenter determination method. We found that six $M \geq 7.0$ events appear to have occurred on segments of the Sumatran fault as follows: Kumering for the 1933 (M_s 7.5) event; the northwestern and southeastern parts of Tripa for the 1935 (M_s 7.0) and 1936 (M_s 7.2) events, respectively; the southeastern half of Sunda for the April 1943 (M_s 7.1) event; Ketaun for the first (M_s 7.3) event of the June 1943 doublet; and Suliti and Sumani for the second (M_s 7.6) event of the June 1943 doublet. We also identified the faults of four $M \geq 7.0$ earthquakes between 1892 and 1920 by using information on crustal deformation and damage distributions. From the results of earthquake locations between 1892 and 2012, and the corresponding fault lengths of $M \geq 7.0$ earthquakes, we have interpreted the large ($M \geq 7.0$) earthquake history of the Sumatran fault for the past 120 years. Possible seismic gaps for $M \geq 7.0$ earthquakes along the Sumatran fault are the northern half of the Sunda segment, and the Semangko, Dikit, Sianok, Barumun, Toru, Renun, Aceh, and Seulimeum segments.

Introduction

Sumatra is located at the plate boundary between the subducting Indian and Australian plates and the overriding Sundaland plate. According to the MORVEL model of DeMets *et al.* (2010), slip rates of the subduction between the Indian and Sundaland plates are 46–48 mm/yr off Sumatra Island (Fig. 1). Because the subduction is oblique, a trench-parallel strike-slip fault, the Sumatran fault, has been generated near the southwestern coast of the Sumatran Island (Fitch, 1972; Fig. 1). The total length of the right-lateral strike-slip Sumatran fault is 1900 km, which Sieh and Natawidjaja (2000) divided into 19 major fault segments. We accept the segments defined by Sieh and Natawidjaja (2000) in this study. Recent Global Positioning System (GPS) observations show that slip rates of the Sumatran fault are 16–20 mm/yr in northern Sumatra (Ito *et al.*, 2012) and 23 mm/yr in central Sumatra (Genrich *et al.*, 2000), whereas Satellite Pour l'Observation de la Terre (SPOT) data (Bellier and Sebrier, 1995) show that the slip rate is 6 mm/yr in southern Sumatra (Fig. 1).

Many shallow right-lateral strike-slip fault earthquakes have occurred along the Sumatran fault in addition to reverse-faulting subduction earthquakes near the Sunda trench (Fig. 1). Seismic activity along the Sumatran fault is high, and many large earthquakes have occurred along the fault. For example, one of the largest earthquakes since 1892 was the second event of the June 1943 doublet (M_s 7.6), following the first event of M_s 7.3. The rupture of this event produced failure of the Sumani segment of the Sumatran fault (Natawidjaja *et al.*, 1995; Sieh and Natawidjaja, 2000), with right-lateral surface offsets of up to 2–3 m (Untung *et al.*, 1985).

Katili and Hehuwat (1967) mapped fault planes of large earthquakes between 1890 and 1952 on the Sumatran fault based on information of crustal deformation and damage distributions by the earthquakes. Earthquake data, however, are limited. Katili and Hehuwat (1967) included only five $M \geq 7.0$ earthquakes and five $M < 7.0$ earthquakes, although they did not mention magnitudes of earthquakes.

Bellier *et al.* (1997) interpreted fault segmentation of the Sumatran fault by reporting major earthquake ruptures on the basis of historical seismicity. The historical record identified 17 earthquakes since 1835 and suggests a northward increase in seismic hazard along the Sumatran fault. Those authors proposed three seismic gaps: S3, S5–S7, and S15–S17, which correspond respectively to the northwestern part of the Kumering segment; to the Ketaun, Dikit, Siulak, and Suliti segments; and to the Tripa and Aceh segments (segment nomenclature follows Sieh and Natawidjaja, 2000). Although Bellier *et al.* (1997) specified the rupture zones of the large earthquakes, the lengths of the rupture zones are inconsistent

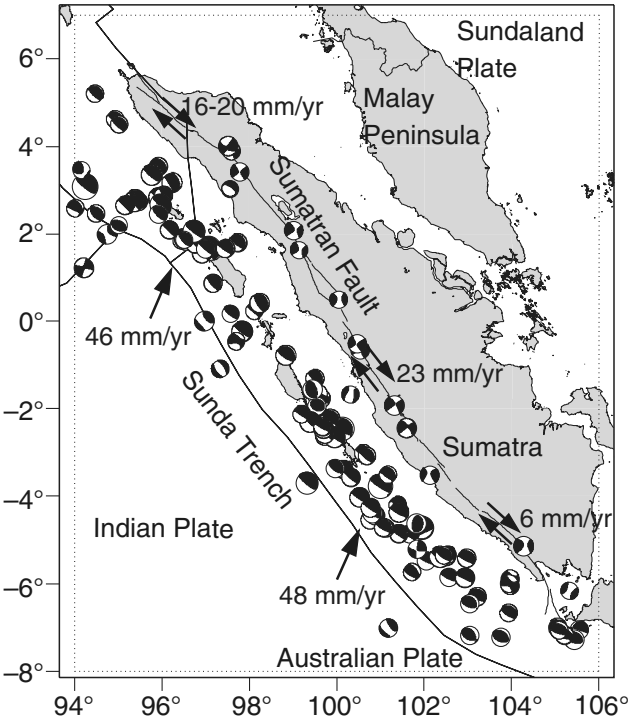

Figure 1. Tectonic setting of Sumatra. The right-lateral strike-slip motion of the Sumatran fault is parallel to the Sunda trench in the Sumatran subduction zone. Slip rates in the figure represent subduction of the Indian plate beneath the Sundaland plate using the MORVEL model (from DeMets *et al.*, 2010). Global Centroid Moment Tensor (CMT) solutions (see Data and Resources) of shallow earthquakes ($M_w \geq 6.0$ and depth ≤ 60 km) between 1976 and 2012 are also plotted. Slip rates of the Sumatran fault in northern, central, and southern Sumatra are taken from Bellier and Sebrier (1995), Genrich *et al.* (2000), and Ito *et al.* (2012), respectively. The configuration of the Sumatran fault is from Sieh and Natawidjaja (2000).

with the magnitudes of some earthquakes. Furthermore, the selection of large earthquakes in their papers is not uniform in earthquake magnitude.

Sieh and Natawidjaja (2000) also studied the relationship between large historical earthquakes since 1822 and fault segments of the Sumatran fault. Among the 19 segments they proposed, no records of large historical earthquakes were found for the Sunda, Dikit, Sumpur, Barumun, or Aceh segments. Natawidjaja and Triyoso (2007) mapped expected source areas of the earthquakes referred to Sieh and Natawidjaja (2000). Similar to Bellier *et al.* (1997), however, the sizes of the source areas of some earthquakes were inconsistent with earthquake magnitudes.

In the northernmost part of the Sumatran fault, neither the Aceh nor the Seulimeum segment has experienced a major earthquake for at least 170 years. Therefore, a seismic gap is considered to be located there (e.g., Bellier *et al.*, 1997; Sorensen and Atakan, 2008). In a recent study of the Aceh segment, which is 200 km long, Ito *et al.* (2012) found a shallow creeping and locked zone that appears to be capable of producing a significant earthquake. Their estimation of locking depth and slip-deficit rate in this segment suggested that the accumulated seismic moment over 170 years corresponds to an earthquake of magnitude (M) 7.

The purposes of this study are as follows: (1) relocating epicenters of all earthquakes along the Sumatran fault precisely with $M \geq 7.0$ from 1892 to 2012, because locations of some earthquakes in existing catalogs are unreliable. We obtain a catalog of large shallow Sumatra earthquakes that are, to a high degree of confidence, located in the overriding Sundaland plate instead of in the Sumatran subduction zone. We identify large earthquakes that are proposed to have occurred on the Sumatran fault but that have not previously been associated with the fault. Furthermore, we explore the extent to which shallow earthquakes in the overriding Sundaland plate occur on faults that are distinct from the Sumatran fault as that fault is currently mapped. (2) Associating the earthquake epicenters with geologically mapped fault segments and identifying the fault planes of these earthquakes. By studying the extent to which seismicity of the Sumatran fault is correlated with segments and segment boundaries, we suggest possible modifications to previously mapped segment boundaries. (3) Obtaining the earthquake history of the Sumatran fault from 1892 to the present by using reliable epicenters and fault planes of the large earthquakes. Finally, (4) detecting seismic gaps along the Sumatran fault to contribute to earthquake disaster mitigation in future.

Some old earthquakes before 1964, when the International Seimological Centre (ISC) was established, are not well located because of the limited number of seismic stations in the region and poor readings of arrival times. Although some studies have relocated old large earthquakes, including those along the Sumatran fault (Newcomb and McCann, 1987; Engdahl and Villaseñor, 2002), not all of the earthquakes concerned were relocated. Recently, a new global instrumental earthquake catalog called ISC-Global Earthquake Model (ISC-GEM) was released (Storchak *et al.*, 2013), which covered the period of 1900–2009. Although locations of old earthquakes were greatly improved, the cutoff magnitude in the period between 1900 and 1917 is M_s 7.5. We compare our locations and those by the International Seismological Summary (ISS) and ISC-GEM under the Results section. Furthermore, because previous studies that identified fault planes of large historical earthquakes used different magnitude scales, the obtained sizes of the faults are both inconsistent and incorrect. Therefore, we need to construct a complete earthquake catalog for the Sumatran fault by using surface-wave magnitude (M_s) as calculated by Abe (1981, 1984) and Abe and Noguchi (1983a,b), who carefully reexamined $M_s \geq 7.0$ earthquakes worldwide between 1897 and 1980. We employed M_w using Global Centroid Moment Tensor (CMT) solutions (see Data and Resources) for earthquakes between 1976 and 2012. On this basis, we are able to obtain the complete earthquake history of the Sumatran fault.

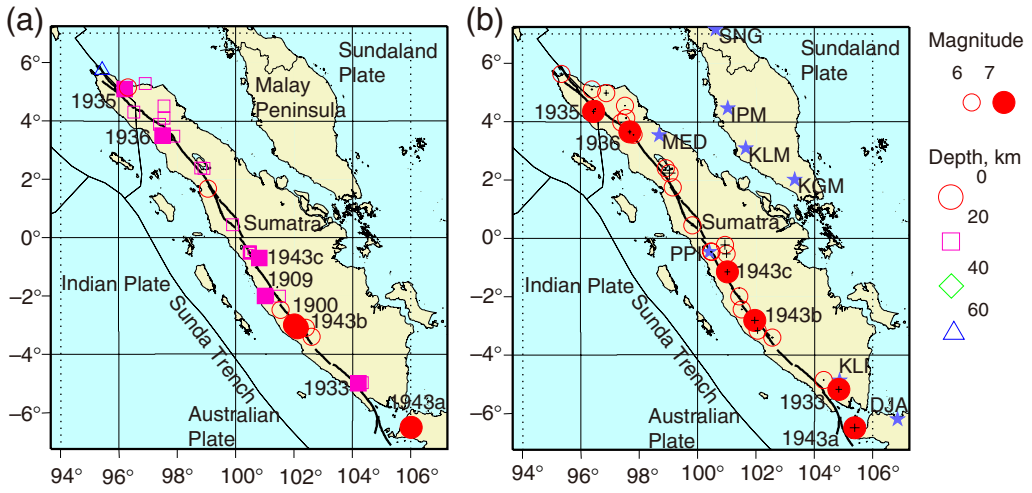

Figure 2. Epicenter distribution of large shallow earthquakes along and near the Sumatran fault since 1900. (a) Hypocenters listed in various catalogs (refer to text). (b) Relocated modified joint hypocenter determination (MJHD) hypocenters in this study. A cross with the circle indicates the standard errors in latitude and longitude. Stations used in the relocation are shown by stars. The Sumatran fault configuration is taken from Sieh and Natawidjaja (2000). The color version of this figure is available only in the electronic edition.

Method and Data

Method

The modified joint hypocenter determination (MJHD) method was used for making precise relocations of large earthquakes along the Sumatran fault. The MJHD method was developed by Hurukawa and Imoto (1990, 1992) for local location and Hurukawa (1995) for global location from the joint hypocenter determination (JHD) method. The JHD method (Douglas, 1967; Freedman, 1967; Dewey, 1972) calculates hypocenters of a group of earthquakes and station corrections simultaneously. Station corrections remove the effects of lateral heterogeneity and reflect the travel-time difference between the assumed 1D velocity model and the actual structure. There is a trade-off, however, between location and station corrections, because when the azimuthal coverage of stations is poor, the solution becomes unstable and unreliable. Hurukawa and Imoto (1990, 1992), Hurukawa (1995), and Hurukawa *et al.* (2008) overcame this problem in the JHD method by adding the constraint that station correction is independent of the distance and azimuth from the center of the source region to each station (equation 1 in Hurukawa *et al.*, 2008). Because, for example, a summation of a product of a station correction and the distance, sine or cosine of the azimuth at each station should be zero, this constraint suppresses the absolute values of station corrections. Although the arrival times of historical earthquakes include large reading or clock errors, the MJHD method can clearly discriminate reading or clock errors from station corrections. In this study, we fixed the focal depths of all earthquakes to 15 km, because data are available only from a small number of stations, especially nearby stations that record historical earthquakes. The underlying assumption of the MJHD approach is that the source–receiver distances are significantly larger than the cluster size (the interevent distances). Thus, the station corrections represent the travel-time effects of unmodeled 3D velocity heterogeneities along repeating ray paths between the stations and the event cluster. Given that this event cluster spans 1900 km, and local/regional stations are also used in the multiple-event location, the above assumption might be violated. If many stations in the Sumatra Island and the Malay Peninsula were available before 1950, it is better to divide the target area into several smaller areas. However, only Medan (MED) station was available there before 1950. The maximum travel-time residual (O−C) allowed in this study is 7 s considering reading errors and small-scale heterogeneity in the target area, although the latter will be much smaller than the former. Concerning recent earthquakes that were observed by many local/regional stations with high accuracy, reading errors will be smaller than effects of the small-scale heterogeneity in the target area. Therefore, their locations may contain bias caused by the effects.

Data

We selected only shallow earthquakes near the Sumatran fault and inland earthquakes in the Sumatra Island, in the area 8° S–7° N and 94° E–106° E (the dotted area in Figs. 1 and 2). For earthquakes after 1976, we selected only strike-slip events by referring to Global CMT solutions (see Data and Resources).

There have been 10 $M \geq 7.0$ earthquakes along the Sumatran fault since 1892 (Table 1). As phase data are available for the period 1900 to present, we tried to relocate the eight $M \geq 7.0$ earthquakes for this period (Fig. 2a). Note that all $M \geq 7.0$ earthquakes occurred before 1944. A number of stations in the period of 1943 were small, and readings of onset times contained large errors including clock errors. To utilize the stations for that interval, we also relocated

Table 1
List of Earthquakes

Date (yyyy/mm/dd)	Time (hh:mm)	Longitude (° E)	Latitude (° N)	Z (km)*	M	Type of M	Source of hypocenter	Source of M
1892/05/17	13:18L†	99.5	0.8	—	7.5	M	Utsu (2002)	Utsu (2002)
1893/06/12	07:57L†	103.0	−4.1	—	7.0	M	This study	This study
1900/01/05	19:00	102.5	−3.5	—	7.0	M_s	This study	AN‡
1909/06/03	18:40	101.0	−2.0	35	7.3	M_s	ISS	AN‡
1921/04/01	04:06	99.03 ± 0.22	2.25 ± 0.23	15	6.8	M	This study	CENT.CAT§
1926/06/28	03:23	100.98 ± 0.15	−0.53 ± 0.14	15	6.8	M	This study	CENT.CAT§
1926/06/28	06:15	100.93 ± 0.16	−0.21 ± 0.17	15	6.5	M	This study	UN‖
1933/06/24	21:54	104.83 ± 0.11	−5.18 ± 0.11	15	7.5	M_s	This study	Abe (1981)
1935/08/03	01:10	96.44 ± 0.06	4.36 ± 0.08	15	7.0	M_s	This study	Abe (1981)
1936/09/19	01:01	97.67 ± 0.06	3.66 ± 0.07	15	7.2	M_s	This study	Abe (1981)
1942/05/24	03:26	96.87 ± 0.09	5.00 ± 0.11	15	6.8	M	This study	CENT.CAT§
1943/04/01	14:18	105.38 ± 0.16	−6.49 ± 0.14	15	7.1	M_s	This study	Abe (1981)
1943/06/08	20:42	101.95 ± 0.13	−2.81 ± 0.12	15	7.3	M_s	This study	Abe (1981)
1943/06/09	03:06	101.02 ± 0.10	−1.15 ± 0.10	15	7.6	M_s	This study	Abe (1981)
1952/03/15	11:15	102.04 ± 0.10	−3.17 ± 0.11	15	6.8	M	This study	BMKG
1964/04/02	01:11	95.33 ± 0.07	5.65 ± 0.05	15	6.7	mb	This study	NEIC
1967/04/12	04:51	96.38 ± 0.04	5.11 ± 0.04	15	6.1	mb	This study	ISC
1977/03/08	23:17	99.81 ± 0.05	0.45 ± 0.04	15	6.1	M_w	This study	Global CMT
1979/12/15	00:02	102.55 ± 0.05	−3.41 ± 0.04	15	6.5	M_w	This study	Global CMT
1980/04/01	16:21	97.55 ± 0.03	4.13 ± 0.03	15	6.0	M_w	This study	Global CMT
1987/04/25	19:22	98.91 ± 0.03	2.41 ± 0.03	15	6.4	M_w	This study	Global CMT
1990/11/15	02:34	97.39 ± 0.02	3.98 ± 0.02	15	6.7	M_w	This study	Global CMT
1994/02/15	17:07	104.31 ± 0.03	−4.85 ± 0.03	15	6.8	M_w	This study	Global CMT
1995/10/06	18:09	101.42 ± 0.03	−1.99 ± 0.03	15	6.7	M_w	This study	Global CMT
1996/10/10	15:21	97.81 ± 0.02	3.56 ± 0.02	15	6.2	M_w	This study	Global CMT
1997/08/20	07:15	96.50 ± 0.03	4.45 ± 0.03	15	6.0	M_w	This study	Global CMT
2003/01/22	02:58	97.51 ± 0.03	4.57 ± 0.02	15	6.0	M_s	This study	ISC
2007/03/06	03:49	100.46 ± 0.04	−0.46 ± 0.03	15	6.4	M_w	This study	Global CMT
2007/03/06	05:49	100.45 ± 0.02	−0.45 ± 0.02	15	6.3	M_w	This study	Global CMT
2008/05/19	14:26	99.14 ± 0.02	1.76 ± 0.02	15	6.0	M_w	This study	Global CMT
2009/10/01	01:52	101.51 ± 0.03	−2.44 ± 0.03	15	6.6	M_w	This study	Global CMT

*Z, depth (fixed for earthquakes after 1921).
†L, local time.
‡AN, Abe and Noguchi (1983b).
§CENT.CAT, Engdahl and Villaseñor (2002).
‖UN, Untung *et al.* (1985).

$6.0 \leq M < 7.0$ earthquakes for the period 1921 to present (Fig. 2a), because common stations that recorded both $M \geq 7.0$ and $M < 7.0$ earthquakes in the period prior to 1944 contribute to improving their locations. Moreover, because recent earthquakes were recorded by many more seismic stations, and with higher reading accuracies than the old earthquakes, these additional data helped to obtain better locations of the pre-1944 earthquakes. Note that the ISS reported some immediate aftershocks of the 1926 and 1933 earthquakes. Because the numbers of available stations are limited, however, we could not include these aftershocks in our relocation.

Only initial *P*-wave arrival times were used in this study, because these are more reliably observed than are the subsequent *S*-wave and later-phase arrival times. The initial *P*-wave arrival times at worldwide stations were taken from various references as follows: 1900–1917, British Association for the Advancement of Science, Seismology Committee; 1918–1963, ISS; 1964–2008, ISC (see Data and Resources); and 2009–2012, U. S. Geological Survey (USGS). We used the iasp91 model (Kennett and Engdahl, 1991) to estimate travel times.

To obtain an earthquake history that includes the locations of fault planes, the size of each large earthquake should be known correctly. Therefore, we used M_s from Abe (1981) and Abe and Noguchi (1983b) for earthquakes $M_s \geq 7.0$ after 1900. We used M_s from the ISC and M_w from Global CMT for earthquakes during 1964–1975 and 1976–2012, respectively. Because these kinds of M were not available for the 1964 and 2003 earthquakes, we used M_s from the National Earthquake Information Center (NEIC) and M_s from the ISC for these events, respectively.

To calculate MJHD hypocenters, two parameters must be defined: the minimum number of stations (MSTN) that observed each earthquake and the minimum number of events (MEVN) observed at each station. Here, MSTN and MEVN were set to 10 and 5, respectively. We added MED station in northern Sumatra, however, where the number of events observed was 4, because it is one of the nearest stations and observed earthquakes between 1933 and 1977. We used 583

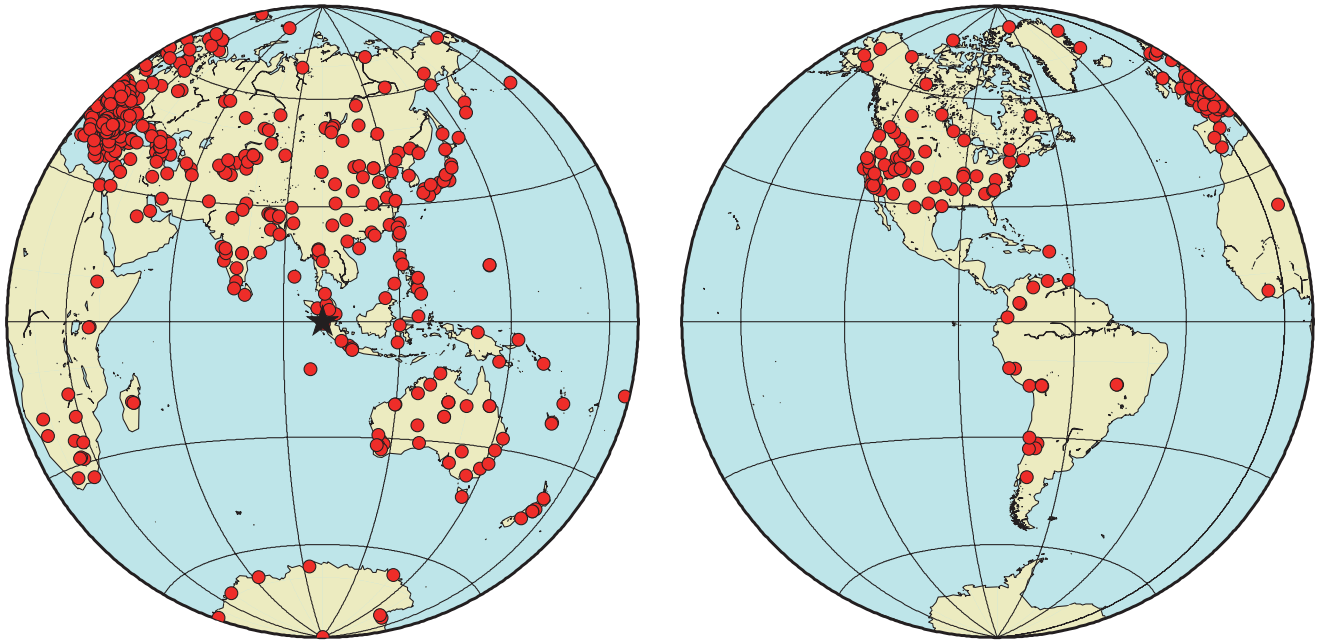

Figure 3. Distribution of seismic stations, in which initial *P*-wave arrival times were used for relocation. The color version of this figure is available only in the electronic edition.

worldwide stations as shown in Figure 3. Phase data with an absolute value of a *P*-wave travel-time residual (O−C, observed minus calculated time) of ≥7 s were excluded.

Results

We were able to relocate 27 $M \geq 6.0$ earthquakes including six $M \geq 7.0$ earthquakes for the period after 1921 (Table 1; Fig. 2b). However, because travel-time residuals of *P*-arrival times for the 1900 (*M* 7.0) and 1909 (*M* 7.3) earthquakes were too large, these earthquakes were excluded from MJHD relocation. Almost all the earthquakes were located on the Sumatran fault. Detailed results for the six $M \geq 7.0$ earthquakes are explained in the next section, along with a discussion of the relationship between the earthquakes and the fault segments of the Sumatran fault (Fig. 4).

We need to know how fault length corresponds to earthquake magnitude in order to identify the corresponding fault segment and to ascertain the seismic gaps where future large earthquakes are expected to occur. Therefore, the fault length for magnitude $M \geq 7.0$ events was estimated using the equation for large earthquakes on the Sagaing fault, which is a similar type of trench-parallel strike-slip fault to the Sumatran fault, but in Myanmar (Hurukawa and Maung, 2011). Hurukawa and Maung (2011) used the surface-wave magnitude M_s of Abe (1981) for $M \geq 7.0$ earthquakes, and the equation is

$$\log(L) = 0.66M - 2.83, \qquad (1)$$

in which *L* is the length of the fault in kilometers and *M* is the earthquake magnitude. From the equation, *M* values of 7.0, 7.3, and 7.6 yielded fault lengths of 62, 97, and 153 km, respectively. Note that the estimates of *L* that were obtained from equation (1) have an associated uncertainty. According to figure 2 of Hurukawa and Maung (2011), the uncertainty will be ∼10% in equation (1). Because a triangulation network detected displacements along the Angkola segment caused by the 1892 *M* 7.5 earthquake (Muller, 1895; Bellier *et al.*, 1997; Prawirodirdjo *et al.*, 2000; Sieh and Natawidjaja, 2000), we used this event as a calibration event for the fault-scaling relation in equation (1). The expected fault length for an *M* 7.5 earthquake is 132 km, which is consistent with the length of the Angkola segment (160 km), and the difference is ∼20%, or about 0.1 magnitude units.

Wells and Coppersmith (1994) obtained the regression relationship of subsurface rupture length (RLD in kilometers) and moment magnitude (M_w) for strike-slip earthquakes as $\log(\text{RLD}) = 0.62M_w - 2.57$. From the equation, M_w values of 7.0, 7.3, and 7.6 yielded subsurface rupture lengths, which might correspond to fault lengths, of 59, 90, and 139 km, respectively. Therefore, the difference between the expected fault lengths obtained by the two equations, equation (1) and the equation of Wells and Coppersmith (1994) above, is less than ∼10%.

There is strong lateral heterogeneity in crust and mantle properties around the Sumatra Island because of the location of the island in the subduction zone. This heterogeneity might have affected the locations of the relocated earthquakes. For example, there are low- and high-velocity anomalies in the upper mantle in southeast Asia and Australia, respectively (e.g., Inoue *et al.*, 1990; Widiyantoro and Van der Hilst, 1997). We compared the station corrections obtained in this study with velocity anomalies obtained by tomographic studies. Station corrections at 24 stations in the southeast Asia

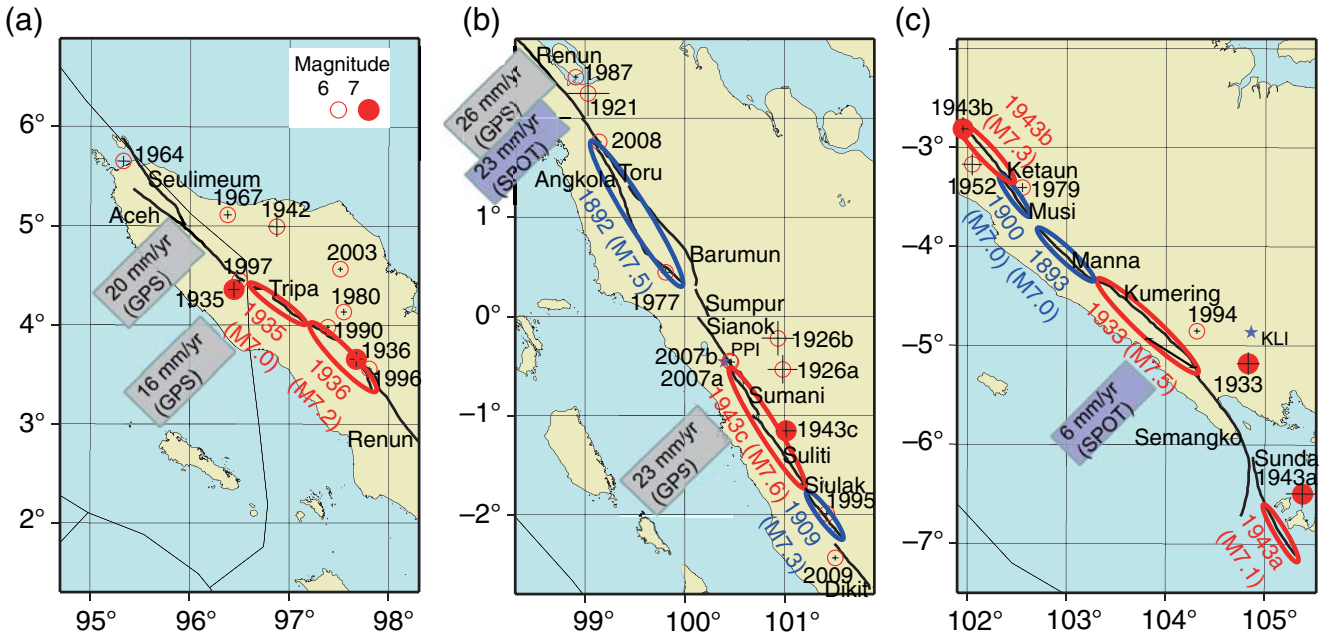

Figure 4. Relocated MJHD epicenters. (a) Northern Sumatra. (b) Central Sumatra. (c) Southern Sumatra. Solid lines with names indicate segments of the Sumatran fault (Sieh and Natawidjaja, 2000). Symbols are as in Figure 2. The thick solid line (see Fig. 4c) indicates the Ranau–Suwoh area, which was severely damaged by the 1933 Liwa earthquake (Berlage, 1934; Widiwijayanti *et al.*, 1996). The slip rates of the Sumatran fault in northern, central, and southern Sumatra are taken from Ito *et al.* (2012) and Genrich *et al.* (2000) for Global Positioning System (GPS) and Bellier and Sebrier (1995) for Satellite Pour l'Observation de la Terre (SPOT). The color version of this figure is available only in the electronic edition.

area (latitude: 0° N–30° N; longitude: 100° E–130° E) and at 29 stations in the Australia area (latitude: 50° S–10° S; longitude: 110° E–150° E) are 2.2 ± 2.1 s and -1.8 ± 1.3 s, respectively. The station corrections are consistent with velocity anomalies in the upper mantle beneath southeast Asia (low V) and Australia (high V). This implies that a significant portion of the effect of the lateral heterogeneity was removed by using the station corrections. However, although local lateral heterogeneity exists beneath Sumatra Island (e.g., Puspito *et al.*, 1993; Widiyantoro and Van der Hilst, 1997), it is very difficult to evaluate its full effect, and therefore the effect of local heterogeneity was not estimated.

The bias in the absolute locations of the group of relocated earthquakes should be assessed because the MJHD method sometimes sacrifices some of the accuracy of absolute locations. Fourteen $M \geq 6.0$ earthquakes have occurred on and around Sumatra Island since 1977 (Table 1). Of these, 12 (excluding the 1980 and 2003 earthquakes) were located very close to the Sumatran fault (Fig. 4). The average distance between the Sumatran fault and the epicenters of 9 of the 12 earthquakes (excluding the 1979, 1987, and 1994 earthquakes) is -0.2 ± 4.8 km (the negative sign indicates that an epicenter is located southwest of the Sumatran fault). Therefore, there is no bias in the direction perpendicular to the fault in the region between ~5° N and ~4° S. The location of the 1994 earthquake is discussed in the 24 June 1933 Liwa Earthquake (M_s 7.5) section. However, it is difficult to evaluate the bias in the direction parallel to the fault. The bias in the locations of relocated earthquakes along the central Sumatran fault is discussed in the 9 June 1943 Padang Highland Earthquake (M_s 7.6) section.

Six $M \geq 7.0$ earthquakes were thought to have occurred along the Sumatran fault. The average distance between the Sumatran fault and the epicenters of these six earthquakes, as reported by the MJHD, ISS, and the ISC-GEM are 16 ± 27, 20 ± 45, and 13 ± 27 km, respectively. Positive values indicate that the average distances are northeast of the Sumatran fault. These results indicate that the MJHD process did not in general produce larger biases than those generated by single-event procedures and that the MJHD and ISC-GEM locations were greatly improved from those by the ISS.

Fault Planes of $M \geq 7.0$ Earthquakes between 1921 and 2012

24 June 1933 Liwa Earthquake (M_s 7.5)

Our epicenter for the Liwa earthquake was located ~50 km northeast of the Semangko segment and ~60 km east of the southern end of the Kumering segment in southern Sumatra (Figs. 2b and 4c). The 1933 Liwa earthquake caused heavy damage in the Ranau–Suwoh area (Berlage, 1934; Widiwijayanti *et al.*, 1996), as outlined by the thick solid line in Figure 4c. Although there is a possibility that a subsidiary fault off the Sumatran fault might have caused the 1933 earthquake, the damage reports suggest that at least the

southern half of the Kumering segment was ruptured during the earthquake.

The 1994 Liwa earthquake (M_w 6.8) was located close to the 1933 event. Carrying out an aftershock study with a temporary network of stations, Widiwijayanti *et al.* (1996) reported that aftershocks of the 1994 earthquake were located in the Ranau–Suwoh area in the southeastern part of the Kumering segment. By comparing the preliminary determination of epicenters NEIC position of the 1994 mainshock relative to the aftershock distribution, Widiwijayanti *et al.* (1996) noted an eastward shift of ~20 km. Furthermore, they inferred that the absolute locations of earthquakes around it were systematically biased 20–50 km eastward. These indicate that our epicenter for the 1994 mainshock is mislocated ~30 km to the east or northeast. Therefore, we suppose that the epicenter of the 1933 earthquake was also mislocated 20–50 km to the east or northeast, similar to the 1994 event. If we correct this mislocation, the mainshock of the 1933 earthquake is situated close to the northwesternmost part of the Semangko or the southeastern end of the Kumering segment. The main reason for these mislocations might be the strong lateral heterogeneity in the crust and mantle beneath Sumatra and its surrounding regions caused by the subduction of the India and Australia plates (e.g., Widiyantoro and Van der Hilst, 1997; Okabe *et al.*, 2004). However, it is difficult to evaluate travel-time anomalies caused by the lateral heterogeneity, because there might be additional small-scale lateral heterogeneities caused by volcanic activity.

The ISS reported five immediate aftershocks of the 1933 earthquake but assumed that the locations of these aftershocks were the same as the location of the mainshock because of limited data. To discover the locations of aftershocks on the Sumatran fault to the epicenter of the mainshock (i.e., northwest or southeast of the mainshock), we plotted relative travel-time differences at common stations between the mainshock and each aftershock. A relative travel-time difference is the difference in arrival times, as measured in seconds, between two events, and in Figure 5 the values of travel-time difference are arbitrarily shifted event-by-event along the axis to prevent overlapping in the figure. Three aftershocks (AF1, AF2, and AF3) were available, as shown in Figure 5. However, the other two aftershocks (AF4 and AF5) were not available because only reasonable arrival times at three stations with similar azimuths were reported by the ISS. For two of the aftershocks (AF2 and AF3), it is clear that relative to the mainshock, relative travel-time differences are larger in the southeast direction than in the northwest direction, indicating that the aftershocks occurred northwest of the mainshock. The maximum differences in the relative travel time (dT), southeast minus northwest, are ~16 and ~10 s for AF2 and AF3, respectively. To convert the time difference to the distance between the mainshock and the aftershocks, we referred to theoretical travel times. Because four stations in AF2 range from ~0.4° to ~11°, in which $dT/d\Delta$ is ~13.7 s/deg, the difference of epicentral distances between the mainshock and AF2 is ~130 km. On the other hand, stations in AF3 range from ~2° to ~72°, in which $dT/d\Delta$ are ~6 to ~14 s/deg, the difference of epicentral distances between the mainshock and AF3 is ~100 km, although the estimation error is large. Therefore, we can conclude that the two aftershocks (AF2 and AF3) of the 1933 earthquake were located ~130 and ~100 km northwest of the mainshock, respectively. From this analysis, it is possible that the rupture extended northwestward for as much as 130 km.

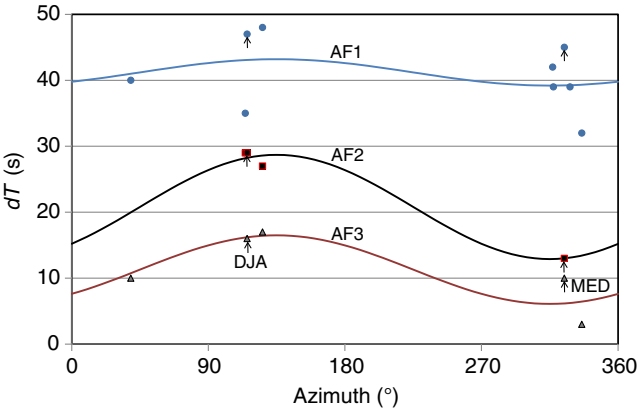

Figure 5. Relative travel-time differences at common stations for the 1933 mainshock and its aftershocks (AF1, AF2, and AF3). The dT plotted is the difference in arrival times, as measured in seconds, between the aftershock and mainshock arrival times with arbitrary shifts. Azimuth is measured from north to east. Arrows indicate data at DJA (Jakarta) and MED (Medan in Sumatra). The dates and origin times of the three aftershocks are as follows: AF1, 5 hr 43 min; AF2, 9 hr 19 min; and AF3, 9 hr 39 min, 25 June 1933. The color version of this figure is available only in the electronic edition.

The expected fault length for an M_s 7.5 earthquake is ~130 km, using equation (1), which is close to the distance between the mainshock and aftershock AF2 (~130 km), and to the length of the Kumering segment (150 km). Therefore, we propose that the 1933 earthquake may have ruptured most of the Kumering segment. Our results are consistent with those of previous studies (e.g., Bellier *et al.*, 1997; Sieh and Natawidjaja, 2000). The rupture was initiated near the southeastern end of the Kumering segment and propagated northwestward to the end of the segment. There is a possibility, however, that the 1933 earthquake initiated at the Semangko segment and ruptured the northeastern part of the Semangko segment and the southwestern part of the Kumering segment. More study is necessary to finalize the location of the earthquake fault.

3 August 1935 Earthquake (M_s 7.0)

This earthquake was relocated near the boundary of the Tripa and Aceh segments in northern Sumatra (Figs. 2b and 4a), whereas the ISS located it near the boundary of the Aceh and Seulimeum segments (Fig. 2a). There are two candidate segments for this earthquake: the Tripa and Aceh segments. We consider the Tripa segment as the fault plane based on the

following reasoning. The 1936 earthquake (M_s 7.2) occurred on the southeastern part of the Tripa segment, as explained in the 19 September 1936 Earthquake (M_s 7.2) section. The 1990 earthquake (M_w 6.7) occurred at the center of the segment near the northwestern end of the fault of the 1936 earthquake. As discussed in the Earthquake History and Seismic Gaps along the Sumatran Fault section, almost all M 6 class earthquakes occurred near boundaries of fault segments, such as the 1996 earthquake (M_w 6.2) and the 1997 earthquake (M_w 6.0) that occurred at the southeastern and northwestern ends of the Tripa segment. We may suppose heterogeneity near the hypocenter of the 1990 earthquake. If we consider that the 1935 earthquake ruptured the northwestern part of the Tripa segment, then the southeastern end of the fault of this earthquake reached the position of the hypocenter of the 1990 earthquake near the center of the Tripa segment. Therefore, we speculate that this earthquake occurred on the northwestern part of the Tripa segment and ruptured southeastward. This idea is consistent with the speculation by Sieh and Natawidjaja (2000) that their Tripa segment might be subdivided on the basis of a jog at 4.0° N and a change in strike at 3.85° N. The fault length expected for an M_s 7.0 earthquake is ~60 km, as given by equation (1), which is much shorter than the length of the Tripa segment (180 km). Note that 180 km corresponds to an M_s 7.7 earthquake. There are no previous studies of this event, and our study is the first attempt to identify the fault plane of the 1935 earthquake on the Sumatran fault. There is a possibility, however, that the 1935 earthquake occurred off the Sumatran fault, because the epicenter was located ~12 km away from the fault. Another candidate fault is the Batee fault located ~17 km east of the epicenter, which is a major right-lateral strike-slip fault that diverges from the boundary between Aceh and Tripa segments southward until the coastline (Sieh and Natawidjaja, 2000). Furthermore, we cannot deny the possibility that the 1935 earthquake ruptured the southeastern part of the Aceh segment. More study is necessary to finalize the location of the earthquake fault.

19 September 1936 Earthquake (M_s 7.2)

This earthquake was located near the boundary of the Tripa and Renun segments in northern Sumatra (Figs. 2b and 4a). Sieh and Natawidjaja (2000) considered that the 1936 earthquake occurred on the Tripa segment, referring to the relocated hypocenter of Newcomb and McCann (1987), which is consistent with our location. Therefore, we consider that this earthquake occurred on the Tripa segment. The expected fault length for an M_s 7.2 earthquake is ~80 km, which is much shorter than the length of the Tripa segment (180 km). Therefore, we propose that the 1936 earthquake ruptured the southeastern half of the Tripa segment. The rupture started near the southeastern end of the segment and propagated northwestward. More recently, two large earthquakes, in 1990 (M_w 6.7) and 1996 (M_w 6.2), occurred near the respective ends of the fault of the 1936 earthquake.

1 April 1943 Earthquake (M_s 7.1)

This earthquake was located near the Sunda segment at the southeastern end of the Sumatran fault in southern Sumatra (1943a in Figs. 2 and 4c), whereas the ISS located it ~100 km east of the Sunda segment. To confirm the MJHD location, we examined the original seismograms at station DJA (Jakarta) in west Java. Although no records of the mainshock were available, we found four aftershocks on 2 April 1943. Because the observed S–P times at DJA are ~23 s, the expected epicentral distance is ~1.7°, which is very close to the calculated epicentral distances of 1.47° and 1.83° given by the MJHD location and the Sunda segment, respectively. This means that the MJHD location satisfies the S–P times at DJA. However, the expected epicentral distance from the ISS location is 0.89° at DJA, which cannot explain the observed S–P times. The expected fault length for an M_s 7.1 earthquake is ~70 km, which is much shorter than the length of the Sunda segment (150 km). Note that 150 km corresponds to an M_s 7.6 earthquake. Therefore, this earthquake might have ruptured the southeastern half of the Sunda segment. There are no previous studies of this event, and ours is the first attempt to identify the fault plane of the April 1943 earthquake on the Sumatran fault. Although Figure 1 shows only reverse-fault earthquakes near the southeastern Sunda segment, both reverse and strike-slip fault events with shallow depths and northeast–southwest P axes occurred there (Global CMT solutions).

8 June 1943 Earthquake (M_s 7.3)

This earthquake was the first event of the June 1943 doublet. The earthquake was located at the northwestern end of the Ketaun segment in southern Sumatra (1943b in Figs. 2b and 4c). Although Sieh and Natawidjaja (2000) considered this earthquake to have occurred at the Suliti segment, this interpretation is inconsistent with locations determined by the ISS, Newcomb and McCann (1987), and the present study. Untung *et al.* (1985) reported that none of the local residents mentioned this earlier event of the 1943 doublet as having occurred near the Suliti segment, whereas the local residents observed fault displacements along the Sumani segment during the second event of the doublet. The expected fault length for an M_s 7.3 earthquake is ~100 km, which is consistent with the length of the Ketaun segment (85 km). Therefore, we propose that this earthquake ruptured the Ketaun segment. Note that 85 km corresponds to an M_s 7.2 earthquake. Another large earthquake with M 6.3 occurred in the central part of the Ketaun segment in 1952 and caused right-lateral movement along the fault (Katili and Hehuwat, 1967).

9 June 1943 Padang Highland Earthquake (M_s 7.6)

The Padang Highland earthquake was the second event of the June 1943 doublet, occurred 6 hr after the first event, and was relocated near the Suliti segment in central Sumatra

(1943c in Figs. 2b and 4b). According to Untung *et al.* (1985), fault displacements were observed for at least 60 km along the Sumani segment by local residents during the earthquake. Although previous studies (e.g., Untung *et al.*, 1985; Bellier *et al.*, 1997) considered that this event occurred only along the Sumani segment, Sieh and Natawidjaja (2000) suggested from the distribution of seismic intensities that the northwestern part of the Suliti segment was ruptured in addition to the Sumani segment. The length of the Sumani segment, 60 km, corresponds to an M_s 7.0 earthquake. The fault length corresponding to an M_s 7.6 earthquake is ~150 km, which is much longer than the length of the Suliti segment (95 km) and of the Sumani segment. The total length of the two segments is 155 km, however, which corresponds well to the expected length of an M_s 7.6 earthquake. Therefore, we propose that this event ruptured both the Suliti and Sumani segments simultaneously. The rupture might have started in the center of the Suliti segment and propagated bidirectionally.

The bias in the absolute locations of relocated earthquakes in central Sumatra, including the 1943 Padang Highland earthquake, should also be assessed. The 2007 doublet occurred ~90 km northwest of the 1943 Padang Highland earthquake. The first and second events of the 2007 doublet ruptured the northern half of the Sumani and the southern part of the Sianok segments, respectively (Natawidjaja *et al.*, 2007). Nakano *et al.* (2010) studied the source model of the 2007 doublet using a waveform inversion analysis of data from a broadband seismograph network in Indonesia. Confirming that the two events of the doublet ruptured the Sumani and Sianok segments, respectively, Nakano *et al.* (2010) obtained the epicenters of the two events as being located ~14 and ~10 km to the south-southeast of our calculated locations. This indicates that there exists an ~10 km north-northwest along-strike bias in our calculated locations along the Sumatran fault in central Sumatra.

Fault Planes of $M \geq 7.0$ Earthquakes between 1892 and 1920

Because we were unable to relocate four $M \geq 7.0$ earthquakes between 1892 and 1920, we identified their fault planes as follows.

17 May 1892 Tapanuli Earthquake (M 7.5)

As we had explained in the Results section, a triangulation network detected displacements caused by the 1892 earthquake along the Angkola segment in central Sumatra (Muller, 1895; Prawirodirdjo *et al.*, 2000). Bellier *et al.* (1997) and Sieh and Natawidjaja (2000) considered that the Tapanuli earthquake ruptured the Angkola segment. The expected fault length for an M 7.5 earthquake is ~130 km, which is consistent with the length of the Angkola segment (160 km). Note that a distance of 160 km corresponds to an M_s 7.6 earthquake. Therefore, we propose that the entire Angkola segment was ruptured by the earthquake (Fig. 4b).

12 June 1893 Earthquake (M 7.0)

As no magnitude is given for this earthquake, which occurred in the Highlands of Benkoelen, southern Sumatra, on 12 June 1893, we estimated it as follows. Visser (1922) reported the radii of shaken areas (r) of five large earthquakes in Sumatra whose radii were more than 400 km. Except for the 1893 earthquake, their magnitudes are given. The radii of the shaken areas of the 1892 (M 7.5), 1900 (M_s 7.0), 1909 (M_s 7.3), and 1921 (M_s 6.8) earthquakes are 1300, 600, 530, and 440 km, respectively. The best-fit relationship between M and r is $\log(r) = 0.54M - 1.05$. Therefore, the expected M for the 1893 earthquake, for which r is 550 km, is 7.0. The epicentral area estimated by Visser (1922) is situated in the Manna segment (Sieh and Natawidjaja, 2000). The expected fault length for an M 7.0 earthquake is ~60 km, as given by equation (1), which is consistent with the length of the Manna segment (85 km). The 85 km length corresponds to an M_s 7.2 earthquake. Therefore, there is a possibility that the Manna segment was ruptured by the 1893 earthquake (Fig. 4c), as Sieh and Natawidjaja (2000) suggested.

5 January 1900 Earthquake (M_s 7.0)

According to Abe (1981), the location of this earthquake was near the first event of the 1943 doublet (M_s 7.3) that ruptured the Ketaun segment (as mentioned in the 8 June 1943 Earthquake (M_s 7.3) section, also see Fig. 2a). The nearest unbroken segments are the Dikit segment to the northwest and the Musi segment to the southeast. Visser (1922) reported that severe damage occurred at Kepahiang (3.6° S, 102.6° E) and at Tebing-Tinggi (3.6° S, 103.1° E), and that the epicentral area extended in a direction trending east-northeast–west-southwest, which is nearly perpendicular to the strike of the Sumatran fault. No other $M \geq 7.0$ earthquakes occurred outside of the Sumatran fault, however. If we consider that the earthquake resulted in the rupture of one of the segments of the Sumatran fault, then the Musi segment might have ruptured, as it is closest to the damaged area. The expected fault length for an M_s 7.0 earthquake is ~60 km, which is consistent with the length of the Musi segment (70 km). Therefore, we propose that the 1900 earthquake ruptured the Musi segment (Fig. 4c), although we cannot deny a possibility that the 1900 earthquake occurred off the Sumatran fault.

6 June 1909 Earthquake (M_s 7.3)

The ISS located this earthquake near the Siulak and Suliti segments (Fig. 2a). Visser (1922) reported that the epicentral area of this earthquake had a length of 40 km and that the center of the area was situated at 2.0° S, 101.5° E, where the Siulak segment is located. Furthermore, most of the regions traversed by the Siulak segment were devastated by the earthquake (Sieh and Natawidjaja, 2000). The fault length

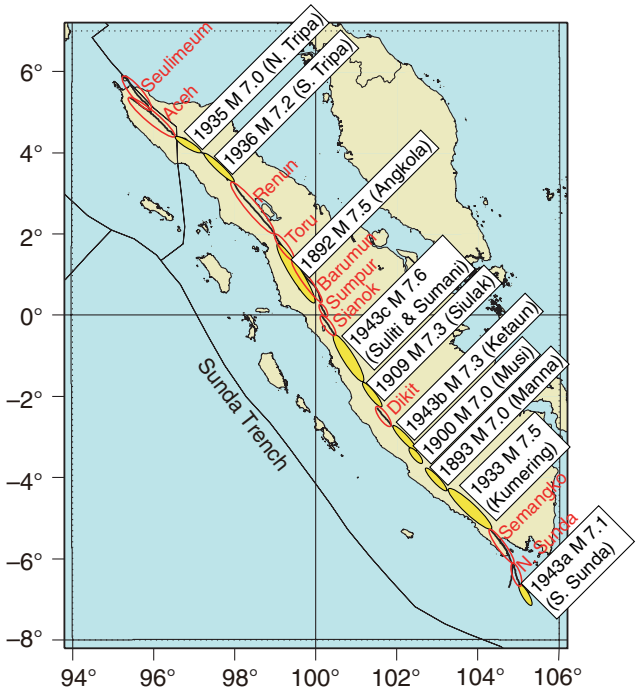

Figure 6. Earthquake history of the Sumatran fault. Filled ellipses indicate $M \geq 7.0$ earthquakes that have occurred since 1892. Open ellipses indicate unbroken fault segments. Names of the Sumatran fault segments are taken from Sieh and Natawidjaja (2000). The color version of this figure is available only in the electronic edition.

expected for an M_s 7.3 earthquake is ~100 km, which is consistent with the length of the Siulak segment (70 km). Note that a length of 70 km corresponds to an M_s 7.1 earthquake. Therefore, we propose that the 1909 earthquake ruptured the Siulak segment (Fig. 4b), similar to Bellier *et al.* (1997) and Sieh and Natawidjaja (2000).

Earthquake History and Seismic Gaps along the Sumatran Fault

To obtain an earthquake history and detect seismic gaps along the Sumatran fault, we plotted the estimated fault planes of all $M \geq 7.0$ earthquakes during 1892–2012 (Fig. 6). The resulting pattern shows seismic gaps along the Sumatran fault, specifically the northeastern part of the Sunda segment, and the Semangko, Dikit, Sianok, Sumpur, Barumun, Toru, Renun, Aceh, and Seulimeum segments. Using equation (1), which defines the relationship between M and fault length, we calculated the maximum magnitude of the expected earthquake in each seismic gap along the Sumatran fault. The expected maximum magnitude is $M \geq 7.0$ for all segments except for the Sumpur (Table 2). Note that if multiple segments rupture simultaneously, similar to the 1943 Padang Highland earthquake, then M will be larger than the equivalent value for a single segment listed in Table 2. The history of $M \geq 6.0$ earthquakes and the seismic gaps of the Sumatran fault are also summarized in Table 2.

These results differ largely from those of Bellier *et al.* (1997) and Sieh and Natawidjaja (2000). The main causes of the differences are attributed to (1) the new findings of the two $M \geq 7.0$ earthquakes (1935 and 1943a), (2) the completeness of the $M \geq 7.0$ earthquake catalog, and (3) the determination and use of proper fault lengths for all earthquakes in our study. We also proposed different fault planes

Table 2
The Sumatran Fault's Major Segments and $M \geq 6.0$ Earthquakes for Period 1892–2012

Number	Segment	Latitude (°)	Length (km)	Large Earthquakes since 1892		M (Max)
				M 7 Class	M 6 Class	
1	Sunda	6.75° S–5.9° S ~	~150	1943a (M 7.1)		7.2 (N. Part)
2	Semangko	5.9° S–5.25° S	65			7.0
3	Kumering	5.3° S–4.35° S	150	1933 (M 7.5)	1994 (M 6.8)	
4	Manna	4.35° S–3.8° S	85	1893 (M 7.0)		
5	Musi	3.65° S–3.25° S	70	1900 (M 7.0)	1979 (M 6.5)	
6	Ketaun	3.35° S–2.75° S	85	1943b (M 7.3)	1952 (M 6.8)	
7	Dikit	2.75° S–2.3° S	60		2009 (M 6.6)	7.0
8	Siulak	2.25° S–1.7° S	70	1909 (M 7.3)	1995 (M 6.7)	
9	Suliti	1.75° S–1.0° S	95	1943c (M 7.6)		
10	Sumani	1.0° S–0.5° S	60	1943c (M 7.6)	1926a (M 6.8), 2007a (M 6.4)	
11	Sianok	0.7° S–0.1° N	90		1926b (M 6.5), 2007b (M 6.3)	7.2
12	Sumpur	0.0° N–0.3° N	35			6.6
13	Barumun	0.3° N–1.2° N	125			7.5
14	Angkola	0.3° N–1.8° N	160	1892 (M 7.5)	1977 (M 6.1)	
15	Toru	1.2° N–2.0° N	95		2008 (M 6.0)	7.3
16	Renun	2.0° N–3.5° N	220		1921 (M 6.8), 1987 (M 6.4)	7.8
17	Tripa	3.4° N–4.4° N	180	1935 (M 7.0), 1936 (M 7.2)	1990 (M 6.7), 1996 (M 6.0),	
18	Aceh	4.4° N–5.4° N	200		1997 (M 6.0)	7.8
19	Seulimeum	5.0° N–5.9° N	120		1964 (M 6.7)	7.4

Segment nomenclature follows Sieh and Natawidjaja (2000).

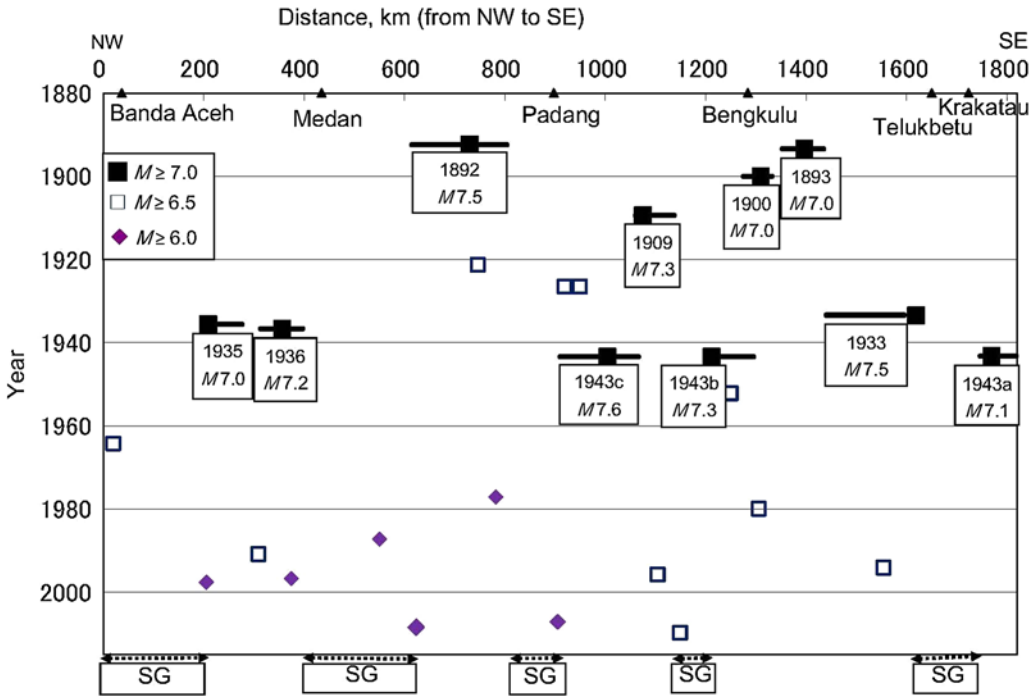

Figure 7. Earthquake history along the Sumatran fault since 1892. Fault planes estimated in this study are shown by thick lines. SG: Seismic gap. The color version of this figure is available only in the electronic edition.

for the following three earthquakes as follows: (1) the 1936 earthquake occurred at the Tripa segment similar to Sieh and Natawidjaja (2000), whereas Bellier *et al.* (1997) considered that it occurred at the Renun segment; the 8 June 1943 (1943b) earthquake occurred at the Ketaun segment, whereas Sieh and Natawidjaja (2000) considered that it occurred at the Suliti segment; and the 9 June 1943 (1943c) earthquake occurred at both Suliti and Sumani segments similar to Sieh and Natawidjaja (2000), whereas Bellier *et al.* (1997) considered that it occurred only at the Sumani segment.

Wells and Coppersmith (1994) obtained the regression relationship of average displacement (AD in meter) and moment magnitude (M_w) for strike-slip earthquakes as $M_w = 7.04 + 0.89 \log(\mathrm{AD})$. This indicates that the expected ADs for M_w 7.0, 7.4, and 7.8 earthquakes are 0.9, 2.5, and 7.1 m, respectively. As shown in Figure 4, slip rates of the Sumatran fault in northern, central, and southern Sumatra are 16–20 mm/yr (Ito *et al.*, 2012), 23–26 mm/yr (Bellier and Sebrier, 1995; Genrich *et al.*, 2000), and 6 mm/yr (Bellier and Sebrier, 1995), respectively. Because the accumulated slip along the fault during the past 120 years has amounted to 1.9–2.4 m in the Aceh and Seulimeum segments, where seismic gaps exist, an $M \leq 7.4$ earthquake might occur in the near future in these locations. As no large earthquakes have occurred in Aceh since at least 1835 (Bellier *et al.*, 1997), more than ~3 m slip has accumulated in the Aceh segment. In the Tripa segment, 1.2–1.5 m of slip has accumulated since the last earthquakes in 1935 and 1936, so that an M 7.0–7.2 earthquake may occur. The Renun segment in central Sumatra has accumulated 2.8–3.1 m during the last 120 years, and ~40% of the stress required for M 7.8 earthquake is already accumulated there. In contrast, the situation in southern Sumatra is different from that of other areas because the slip rate is lower. The accumulated slip amounts to ~0.7 m over the last 120 years, and therefore the possibility of $M \geq 7.0$ earthquakes occurring at historically broken segments in southern Sumatra may be relatively lower than the other region for the near future. Because the last earthquake at each seismic gap and the recurrence interval of the earthquake at each segment are unknown, however, it is impossible to evaluate a probability of the earthquake occurrence at each segment. Therefore, it is quite important to carry out paleoseismological and geomorphological studies of the Sumatran fault including trenching.

A time-versus-space plot of $M \geq 6.0$ earthquakes along the Sumatran fault since 1892 (Fig. 7) clearly shows two active periods of $M \geq 7.0$ earthquakes; namely, 1892–1909 and 1933–1943. Furthermore, many $6.0 \leq M < 7.0$ earthquakes occurred at the same segments where $M \geq 7.0$ earthquakes had previously occurred (see Table 2). For example, the 1994 Liwa earthquake (M 6.8) occurred in the southeastern part of the Kumering segment (Duquesnoy *et al.*, 1996; Widiwijayanti *et al.*, 1996), where the 1933 Liwa earthquake had previously occurred. Another example is the first event (M 6.4) of the 2007 doublet. This event took place in the northwestern part of the Sumani segment (Nakano *et al.*, 2010; Daryono *et al.*, 2012), where the 1943 Padang Highland earthquake had previously occurred. Furthermore, the northwestern part of the Sumani segment was ruptured by the first event (M 6.8) of the 1926 doublet (Untung *et al.*, 1985; Prawirodirjo *et al.*, 2000; Daryono *et al.*, 2012), prior

to the June 1943 earthquake. Therefore, earthquakes of M 6 class may potentially occur along all parts of the Sumatran fault on Sumatra Island, especially near segment boundaries.

Finally, we note that four shallow $6.0 \leq M < 7.0$ earthquakes occurred off the Sumatran fault between 4.0° N and 5.5° N in northern Sumatra, as shown in Figure 4a. These are the 1942 (M 6.8), 1967 (M 6.1), 1980 (M 6.0), and 2003 (M 6.0) earthquakes. No such $M \geq 6.0$ earthquakes, however, occurred in central and southern Sumatra. This implies a high seismic hazard over the entire northern part of Sumatra Island, whereas a high long-term hazard may be restricted to regions near the Sumatran fault in central and southern Sumatra.

Conclusions

We relocated six earthquakes of $M \geq 7.0$ that occurred along or near the Sumatran fault in Sumatra, western Indonesia, since 1921 by using the MJHD method. We added $M \geq 6.0$ earthquakes that took place during 1921–2012 in this relocation. By combining better quality recent data with poorer old ones helped to constrain the locations of pre-1950 earthquakes. We found that six $M \geq 7.0$ earthquakes had occurred along the Sumatran fault and proposed their fault planes and the corresponding fault segments.

The 1933 Liwa earthquake (M_s 7.5) was initiated near the southeastern end of the Kumering segment in southern Sumatra, and the rupture propagated northwestward to the end of the segment. The 1935 (M_s 7.0) earthquake was initiated at the northwestern end of the Tripa segment in northern Sumatra and ruptured toward the southeast to the segment center, whereas the 1936 (M_s 7.2) event was initiated at the southeastern end and ruptured toward the northwest, to the center of the segment. However, we cannot deny a possibility that the 1935 earthquake occurred along the Batee fault because of the uncertainty of the location. The April 1943 (M_s 7.0) earthquake might have ruptured the southeastern part of the Sunda segment in the Sunda Straight. A doublet occurred in central and southern Sumatra in June 1943. The first event (M_s 7.3) of the doublet ruptured the Ketaun segment from northwest to southeast, whereas the second event (M_s 7.6), known as the Padang Highland earthquake, initiated at the Suliti segment and ruptured the Suliti and Sumani segments simultaneously.

We also proposed that the 1900 (M_s 7.0) earthquake had ruptured the Musi segment based on the damage distribution and the fault planes of other $M \geq 7.0$ earthquakes. We cannot deny a possibility, however, that the 1900 earthquake did not occur along the Sumatran fault because of the damage reports off the fault. There were three more $M \geq 7.0$ earthquakes between 1892 and 1920, fault planes of which had already been identified by using information on crustal deformation and damage distributions. From the results of earthquake locations for the period 1892–2012 and the corresponding fault lengths for $M \geq 7.0$ earthquakes, we obtained the history of earthquakes along the Sumatran fault. Possible seismic gaps, where no $M \geq 7.0$ earthquakes have occurred in at least the last 120 years, along the Sumatran fault and corresponding maximum M_s are the northern half of the Sunda segment (M_s 7.2), and the Semangko (M_s 7.0), Dikit (M_s 7.0), Sianok (M_s 7.2), Barumun (M_s 7.5), Toru (M_s 7.3), Renun (M_s 7.8), Aceh (M_s 7.8), and Seulimeum (M_s 7.4) segments. Among these segments, the Aceh and Seulimeum segments, where the slip rate is high, have already accumulated the strain corresponding to $M_s \sim 7.4$ earthquakes.

Data and Resources

Phase data come from Shide Circulars (Schweitzer and Lee, 2003) and Bulletin Disks 1–20 by International Seismological Centre (2012). The Global Centroid Moment Tensor Project database was searched using www.globalcmt.org/CMTsearch.html (last accessed April 2013). The International Seimological Centre-Global Earthquake Model Global Instrumental Earthquake Catalog (Storchak *et al.*, 2013) was also used. Some plots were made using the Generic Mapping Tools version 3.4.5 (Wessel and Smith, 1995).

Acknowledgments

We thank D. Storchak and A. Villaseñor, who provided us with digital International Seismological Summary (ISS) data, and D. H. Natawidjaja for helpful discussions. We thank anonymous reviewers and associate editors for their helpful comments during review. We are grateful to the Agency for Meteorology, Climatology, and Geophysics (BMKG) in Indonesia for permitting us to use old seismograms.

References

Abe, K. (1981). Magnitudes of large shallow earthquakes from 1904 to 1980, *Phys. Earth Planet. In.* **27,** 72–92.

Abe, K. (1984). Complements to "Magnitudes of large shallow earthquakes from 1904 to 1980", *Phys. Earth Planet. In.* **34,** 17–23.

Abe, K., and S. Noguchi (1983a). Determination of magnitude for large shallow earthquakes 1898–1917, *Phys. Earth Planet. In.* **32,** 45–59.

Abe, K., and S. Noguchi (1983b). Revision of magnitudes of large shallow earthquakes, 1897–1912, *Phys. Earth Planet. In.* **33,** 1–11.

Berlage, H., Jr. (1934). De aardbeving zuid Sumatra van 25 Juni 1933: Waarremingen in het epicentrale gebied, *Natuurwet. Tijdschr. Ned. Indie* **94,** 15–36 (in Dutch).

Bellier, O., and M. Sebrier (1995). Is the slip rate variation on the Great Sumatran Fault accommodated by fore-arc stretching, *Geophys. Res. Lett.* **22,** no. 15, 1969–1972.

Bellier, O., M. Sébrier, S. Pramumijoyo, Th. Beaudouin, H. Harjono, I. Bahar, and O. Forni (1997). Paleoseimicity and seismic hazard along the Great Sumatran Fault (Indonesia), *J. Geodyn.* **24,** nos. 1/4, 169–183.

Daryono, M. R., D. H. Natawidjaja, and K. Sieh (2012). Twin-surface ruptures of the March 2007 M > 6 earthquake doublet on the Sumatran Fault, *Bull. Seismol. Soc. Am.* **102,** no. 6, 2356–2367.

DeMets, C., R. G. Gordon, and D. F. Argus (2010). Geologically current plate motions, *Geophys. J. Int.* **181,** 1–80, doi: 10.1111/j.1365-246X.2009.04491.x.

Dewey, J. W. (1972). Seismicity and tectonics of western Venezuela, *Bull. Seismol. Soc. Am.* **62,** no. 6, 1711–1751.

Douglas, A. (1967). Joint epicenter determination, *Nature* **215,** 47–48.

Duquesnoy, Th., O. Bellier, M. Kasser, M. Sebrier, Ch. Vigny, and I. Bahar (1996). Deformation related to the 1994 Liwa earthquake derived from geodetic measurements, *Geophys. Res. Lett.* **23,** no. 21, 3055–3058.

Engdahl, E. R., and A. Villaseñor (2002). Global seismicity: 1900–1999, in *International Handbook of Earthquake and Engineering Seismology Part A*, W. K. Lee, H. Kanamori, P. C. Jennings, and C. Kisslinger (Editors), 665–690.

Fitch, T. (1972). Plate convergence, transcurrent faults, and internal deformation adjacent to southeast Asia and the western Pacific, *J. Geophys. Res.* **77,** 4432–4462.

Freedman, H. W. (1967). A statistical discussion of P residuals from explosions part II, *Bull. Seismol. Soc. Am.* **57,** no. 3, 545–561.

Genrich, J. F., Y. Bock, R. McCaffrey, L. Prawirodirdjo, C. W. Stevens, S. S. O. Puntodewo, C. Subarya, and S. Wdowinski (2000). Distribution of slip at the northern Sumatran fault system, *J. Geophys. Res.* **105,** no. B12, 28,327–28,341.

Hurukawa, N. (1995). Quick aftershock relocation of the 1994 Shikotan earthquake and its fault planes, *Geophys. Res. Lett.* **22,** no. 23, 3159–3162.

Hurukawa, N., and M. Imoto (1990). Fine structure of an underground boundary between the Philippine Sea and Pacific plates beneath the Kanto district, Japan, *Zisin* **43,** 413–429 (in Japanese with English abstract).

Hurukawa, N., and M. Imoto (1992). Subducting oceanic crusts of the Philipine Sea and Pacific plates and weak-zone-normal compression in the Kanto district, Japan, *Geophys. J. Int.* **109,** 639–652.

Hurukawa, N., and P. M. Maung (2011). Two seismic gaps on the Sagaing Fault, Myanmar, derived from relocation of historical earthquakes since 1918, *Geophys. Res. Lett.* **38,** L01310, doi: 10.1029/2010GL046099.

Hurukawa, N., M. Popa, and M. Radulian (2008). Relocation of larger intermediate-depth earthquakes of the Vrancea region, Romania, since 1934 and a seismic gap, *Earth Planets Space* **60,** 565–572.

Inoue, H., Y. Fukao, K. Tanabe, and Y. Ogata (1990). Whole mantle *P*-wave travel time tomography, *Phys. Earth Planet. In.* **59,** 294–328.

International Seismological Centre (2012). Bulletin Disks 1-20 [CD-ROM], International Seismological Centre, Thatcham, United Kingdom.

Ito, T., E. Gunawan, F. Kimata, T. Tabei, M. Simons, I. Meilano, A. Agustan, Y. Ohta, I. Nurdin, and D. Sugiyanto (2012). Isolating along-strike varitions in the depth extent of shallow creep and fault locking on the northern Great Sumatran Fault, *J. Geophys. Res.* **117,** no. B06409, doi: 10.1029/2011JB008940.

Katili, J. A., and F. Hehuwat (1967). On the occurrence of large transcurrent faults in Sumatra, Indonesia, *J. Geosci., Osaka City Uni.* **10,** 5–17.

Kennett, B. L. N., and E. R. Engdahl (1991). Travel times for global earthquake location and phase association, *Geophys. J. Int.* **105,** 429–465.

Muller, J. J. A. (1895). De verplaasting van eenige traiangulatie pilaren in de residentie Tapanuli (Sumatra) tengevoge de aardbeving van 17 Mei 1892, *Natuurwet. Tijdscht. Ned. Indie.* **54,** 299–307 (in Dutch).

Nakano, M., H. Kumagai, S. Toda, R. Ando, T. Yamashina, H. Inoue, and Sunarjo (2010). Source model of an earthquake doublet that occurred in a pull-apart basin along Sumatran fault, Indonesia, *Geophys. J. Int.* **181,** 141–153.

Natawidjaja, D. H., and W. Triyoso (2007). The Sumatran fault zone—From source to hazard, *J. Earthq. Tsunami* **1,** no. 1, 21–47.

Natawidjaja, D., Y. Kumoro, and J. Suprijanto (1995). Gempa bumi tektonik di daerah Bukit tinggi—Muaralabuh: hubungan segmentasi sesar aktif dengan gempa bumi tabun 1926 dan 1943, in paper presented at *Annual Convention*, Geoteknologi-LIPI, Bandung, Indonesia.

Natawidjaja, D. H., A. Tohari, E. Subowo, and M. R. Daryono (2007). Western Sumatra earthquakes of March 6, 2007, Report #1, *EERI Special Earthq. Report* 1–5.

Newcomb, K. R., and W. R. McCann (1987). Seismic history and seismotectonics of the Sunda Arc, *J. Geophys. Res.* **92,** no. B1, 421–439.

Okabe, A., S. Kaneshima, K. Kanjo, T. Ohtaki, and I. Purwana (2004). Surface wave tomography for southeastern Asia using IRIS-FARM and JISNET data, *Phys. Earth Planet. In.* **146,** 101–112.

Prawirodirdjo, L., Y. Bock, and J. F. Genrich (2000). One century of tectonic deformation along the Sumatran fault from triangulation and Global Positioning System surveys, *J. Geophys. Res.* **105,** no. B12, 28,343–28,361.

Puspito, N. T., Y. Yamanaka, T. Miyatake, K. Shimazaki, and K. Hirahara (1993). Three-dimensional *P*-wave velocity structure beneath the Indonesian region, *Tectonophys.* **220,** 175–192.

Schweitzer, J., and W. H. K. Lee (2003). Old seismic bulletins to 1920: A collective heritage from early seismologists, *The International Handbook of Earthquake and Engineering Seismology Part B*, W. H. K. Lee, H. Kanamori, P. C. Jennings, and C. Kisslinger (Editors), Academic Press, London.

Sieh, K., and D. Natawidjaja (2000). Neotectonics of the Sumatran Fault, Indonesia, *J. Geophys. Res.* **105,** no. B12, 28,295–28,326.

Sorensen, M. B., and K. Atakan (2008). Continued earthquake hazard in Northern Sumatra, *Eos Trans. AGU* **89,** no. 14, 133–134.

Storchak, D. A., D. Di Giacomo, I. Bondár, E. R. Engdahl, J. Harris, W. H. K. Lee, A. Villaseñor, and P. Bormann (2013). Public release of the ISC-GEM global instrumental earthquake catalogue (1900–2009), *Seismol. Res. Lett.* **84,** 810–815.

Untung, M., N. Buyung, E. Kertapati, Undang, and C. R. Allen (1985). Rupture along the Great Sumatran Fault, Indonesia, during the earthquakes of 1926 and 1943, *Bull. Seismol. Soc. Am.* **75,** no. 1, 313–317.

Utsu, T. (2002). A list of deadly earthquakes in the world: 1500–2000, in *International Handbook of Earthquake and Engineering Seismology Part A*, W. K. Lee, H. Kanamori, P. C. Jennings, and C. Kisslinger, Academic Press, San Diego, California, 691–717.

Visser, S. (1922). Inland and submarine epicentra of Sumatra and Java earthquakes, *koninklijk Magnetisch en Meteorologisch Observatorium te Batavia* **9,** 1–14.

Wells, D. L., and K. J. Coppersmith (1994). New empirical relationships among magnitude, rupture length, rupture width, rupture area, and surface displacement, *Bull. Seismol. Soc. Am.* **84,** no. 4, 974–1002.

Wessel, P., and W. H. F. Smith (1995). A new version of the Generic Mapping Tools (GMT), *Eos Trans. AGU* **76,** 329.

Widiwijayanti, C., J. Deverchere, R. Louat, M. Sebrier, H. Harjono, M. Diament, and D. Hidayat (1996). Aftershock sequence of the 1994, M_w 6.8, Liwa earthquake (Indonesia): Seismic rupture process in a volcanic arc, *Geophys. Res. Lett.* **23,** no. 21, 3051–3054.

Widiyantoro, S., and R. Van der Hilst (1997). Mantle structure beneath Indonesia inferred from high-resolution tomographic imaging, *Geophys. J. Int.* **130,** 167–182.

Building Research Institute
1 Tachihara, Tsukuba
Ibaraki 305-0802, Japan
hurukawa@kenken.go.jp
(N.H.)

Earthquake Information and Tsunami Division
Agency for Meteorology, Climatology and Geophysics
Jalan Angkasa I No. 2 Kemayoran
Jakarta Pusat, Indonesia
biana.wulandari@gmail.com
(B.R.W.)

Hokkaido University
Kita 10 Nishi 8, Kita-ku
Sapporo 060-0810, Japan
mkasa@mail.sci.hokudai.ac.jp
(M.K.)

Manuscript received 29 July 2013;
Published Online 24 June 2014